AGU PUBLICATIONS

Earth and Space Science

RESEARCH ARTICLE
10.1002/2016EA000181

Key Points:
- The climatological relationship between the diurnal migration of rainfall and ambient wind is clarified
- The diurnal characteristics of rainfall-system migration depend systematically on the background wind
- Advection by background wind is suggested to be an important component of the diurnal rainfall propagation mechanism

Correspondence to:
A. Yanase,
yanase@satellite.isee.nagoya-u.ac.jp

Citation:
Yanase, A., K. Yasunaga, and H. Masunaga (2016), Relationship between the direction of diurnal rainfall migration and the ambient wind over the Southern Sumatra Island, *Earth and Space Science*, *4*, doi:10.1002/2016EA000181.

Received 16 MAY 2016
Accepted 23 DEC 2016
Accepted article online 29 DEC 2016

Relationship between the direction of diurnal rainfall migration and the ambient wind over the Southern Sumatra Island

A. Yanase[1], K. Yasunaga[2,3], and H. Masunaga[4]

[1]Graduate School of Environmental Studies, Nagoya University, Nagoya, Japan, [2]Department of Earth Science, University of Toyama, Toyama, Japan, [3]Japan Agency for Marine-Earth Science and Technology, Yokosuka, Japan, [4]Institute for Space-Earth Environmental Research, Nagoya University, Nagoya, Japan

Abstract This study investigates the climatological relationship between diurnal rainfall migration and the ambient wind over the southern Sumatra by using observation and reanalysis of 15 years of data from the Tropical Rainfall Measuring Mission satellite precipitation radar. When winds in the lower troposphere (1000–500 hPa) are westerly, convective rainfall systems migrate eastward, while rainfall systems dominated by stratiform precipitation propagate to the west in association with mid-upper level easterly winds. When the winds are easterly throughout the troposphere, both convective and stratiform precipitation systems propagate only to the west. Rainfall system migration appears to be generally consistent with ambient zonal wind. It is suggested that the advection by background wind is, in general, a dominant component of the propagation mechanism of diurnal rainfall.

1. Introduction

The Maritime Continent (MC) is a unique region between the Indian and Pacific Oceans (warm pool), consisting of many islands surrounded by warm water. The MC is known as a region of especially high convective activity, and latent heat released from active convection there plays an important role in driving atmospheric general circulation [*Ramage*, 1968; *Neale and Slingo*, 2003]. Over the MC, the diurnal precipitation cycle is one of the most dominant variations among a broad range of time scales of convective activity, ranging from several hours to a year. Accordingly, diurnal variations of rainfall over the MC have drawn great climatological interest for several decades [*Hendon and Woodberry*, 1993; *Nitta and Sekine*, 1994; *Yang and Slingo*, 2001; *Kikuchi and Wang*, 2008]. Many features of these variations have been well documented to date, e.g., the initiation of convection in a mountainous area in the afternoon, the peak of rainfall early in the night, and the movement of rain areas from the mountains to coast or offshore areas around midnight [*Nitta and Sekine*, 1994; *Nesbitt and Zipser*, 2003; *Mori et al.*, 2004; *Sakurai et al.*, 2005; *Ichikawa and Yasunari*, 2006; *Love et al.*, 2011]. However, several fundamental issues still remain unexplained, such as the offshore shift mechanism, interactions with large-scale (longer-period) variations, and local orography effects, although they have been discussed by some previous studies [*Ohsawa et al.*, 2001; *Mapes et al.*, 2003; *Ichikawa and Yasunari*, 2008; *Wu et al.*, 2009]. Owing to our poor understanding of diurnal rainfall variation, current state-of-the-art general circulation models, which are used for weather forecasting and climate projection, still have difficulty reproducing the diurnal precipitation cycle (e.g., amplitude and phase of rainfall).

This study focuses on the migration of precipitation systems, which is among the unresolved issues in the diurnal rainfall cycle over the MC. The relevant processes reported in previous studies include land breeze convergence [*Houze et al.*, 1981], advection by background wind [*Mori et al.*, 2004; *Sakurai et al.*, 2009, 2011], self-replication of convective cells [*Sakurai et al.*, 2009, 2011], convergence of cold outflows produced by rainfall systems [*Fujita et al.*, 2010], and gravity waves triggered by daytime heating of the mixed layer on land [*Mapes et al.*, 2003] or convection on land [*Love et al.*, 2011].

Southwest Sumatra is a suitable location for investigating precipitation system migration. Above all, clear seasonal variations of diurnal cloud and precipitation systems are present in this region. Diurnal cloud system migration and its seasonality, associated with the ambient wind, over Sumatra Island have been investigated by *Sakurai et al.* [2005], as described below. Moreover, diurnal rainfall cycles show clear seasonal contrasts over southern Sumatra Island in Figure 1: an inland peak in the boreal winter (Figure 1a) and an offshore peak in the boreal summer (Figure 1b). Hence, this region offers an ideal test bed to investigate the potential

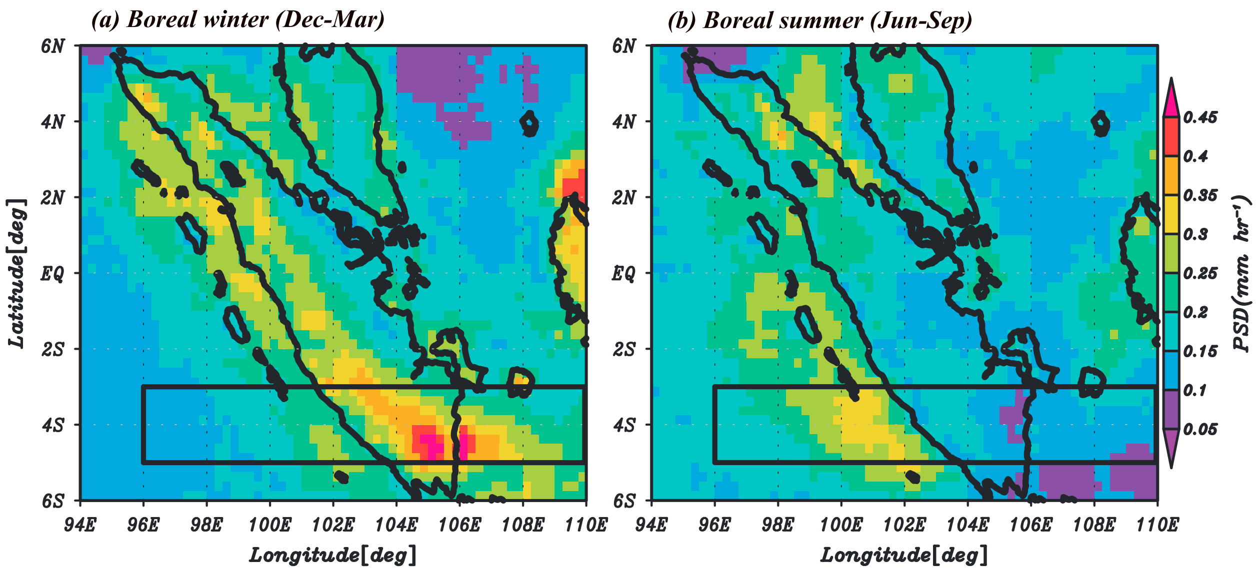

Figure 1. The geographical distribution of the square root of power spectrum density (i.e., amplitude) corresponding to the diurnal cycle calculated by applying the fast Fourier transform (FFT) method to TRMM 3B42 rainfall data in (a) boreal winter and (b) boreal summer. The rectangular area in the panels indicates the analysis domain of this study.

effects of seasonality on the diurnal propagation of precipitation systems. Furthermore, there are no small islands off the coast that could potentially modulate rainfall system propagation, and the region's topography is relatively simple. Thus, we focus on Sumatra Island and its vicinity to explore the migration mechanisms.

Sakurai et al. [2005] revealed seasonal variations in diurnal cloud system migration over Sumatra Island, making use of blackbody temperature (T_{BB}) data from the Geostationary Meteorological Satellite. A westward cloud migration occurs in almost all months over southern Sumatra Island because easterly wind dominates throughout the year in the upper troposphere. On the other hand, eastward cloud migration exists only when the low-level tropospheric wind is westerly. Although they discussed seasonality with focus on the monthly averaged zonal wind, lower troposphere wind direction varies each month. Note that T_{BB} data as a proxy of cloud top temperature are not always a reliable measure of precipitation system migration as an extended area of upper level cirrus veils lower level convection.

Mori et al. [2004] looked into the diurnal cycle of rainfall over Sumatra Island by using Tropical Rainfall Measuring Mission (TRMM) satellite precipitation radar (PR) data and intensive radiosonde soundings. Rainfall systems develop along the southwestern foot of the mountains and propagate to the east or west. The propagation mechanisms, although discussed by *Mori et al*. [2004], remain not entirely clear. It is partly because *Mori et al*. [2004] analyzed a transient period of seasonality (November), when zonal wind direction fluctuates in the lower troposphere.

From a case study using Geostationary Operational Environmental Satellite (GOES-9) and observational data in the first campaign of the Coupling Processes in the Equatorial Atmosphere (CPEA-I) project, the migration direction and speed of convective systems with precipitation were found to be related to the direction and speed of horizontal winds in the lower troposphere [*Sakurai et al*., 2009]. They suggested that the rainfall migration is explained by a self-replication of convective cells and advection caused by the background wind in the lower troposphere. The analysis period of the case study is limited to April and May 2004. Hence, the robustness is not clear because the lower tropospheric zonal wind seasonally varies in direction.

Therefore, further investigation with an extended period of time is needed to clarify the climatological relationship between the ambient wind and rainfall system migration and to test and further elaborate existing hypotheses in order to explain the propagation mechanism. In this study, we examined seasonal changes of the propagation features of the diurnal rainfall by making use of long-term (15 years) observations from TRMM-PR and reanalysis data. In particular, the purpose of our study is to shed light on the potential roles of the direction and magnitude of the ambient wind in the migration of diurnal rainfall.

The data and composite analysis method are described in section 2, and the results from the composite analysis are presented in section 3. Section 4 is devoted to discussion on the results, and a summary is given in section 5.

2. Data and Methodology

2.1. Data

We utilized two TRMM-PR products in this study's composite analysis (TRMM 2A25 version 7 and 3G68). TRMM-PR was the first space borne rain radar, and it could directly observe the three-dimensional structure of precipitation systems. The TRMM 2A25 product contains the surface rainfall rate and vertical distributions of attenuation-corrected reflectivity factor and rainfall rate retrieved from its reflectivity. It also includes the classification of rain types (stratiform, convective, and others) based on the existence of bright band or horizontal homogeneity of radar echoes at the surface. In our analysis, the data were compiled into an hourly gridded product (0.25° × 0.25° spatial resolution) from 1 January 1998 to 31 December 2012.

It takes several days for the TRMM-PR data to recur to the same location. This is because the TRMM satellite completed about 16 orbits per day and the PR instrument had a swath width of only 215 km (247 km after 23 August 2001). To confirm the influence of the infrequent sampling, we used the TRMM 3G68 data product as a supplement in our analysis. TRMM 3G68 is an hourly gridded product (0.25° × 0.25° spatial resolution) that contains rain rate estimates at the surface from the TRMM 2A12 data product, making use of a retrieval algorithm for the TRMM Microwave Imager (TMI) and TRMM-PR (2A25). Although we used both the PR and TMI data, the results using TMI data were consistent with the outcomes using PR data and did not alter the conclusions; thus, we do not show them in this paper.

TRMM 3B42 version 7 is also used in the fast Fourier transform (FFT) analysis in section 1. TRMM 3B42 provides gridded rain rate by using microwave and IR estimation with gauge adjustment, with a 3 h temporal resolution and a 0.25° × 0.25° spatial resolution. The power spectrum density corresponding to the diurnal cycle of rain rate is computed by applying an FFT method using the TRMM 3B42 product from January 1998 to December 2012.

For ambient wind information, we use reanalysis data, known as ERA Interim products, offered by the European Centre for Medium-Range Weather Forecasts (ECMWF). The time resolution of the ERA Interim product is 6 h, and its horizontal-grid interval is 0.75°. We acquired the data spanning from 1 January 1998 to 31 December 2012 to match the temporal coverage of TRMM products. The 6 h wind data are averaged to daily wind, and a 5 day running mean is applied to the daily wind time series to smooth out short-term fluctuations.

2.2. Methodology

We focused on the southern Sumatra Island area described in section 1. The domain for the composite analysis is indicated by the rectangular area (96°E–110°E, 5°S–3°S) in Figure 1, where two separate peaks are found in the onshore (boreal winter, Figure 1a) and offshore (boreal summer, Figure 1b) regions.

Figure 2a shows that the time series of zonal wind averaged for lower troposphere (1000–500 hPa) over the rectangular domain of Figure 1. The temporal mean of the time series is $\bar{U} = 0.4\ \mathrm{m\ s^{-1}}$, and its standard deviation is $\sigma = 3.8\ \mathrm{m\ s^{-1}}$. Using these values, we identify four regimes and make a composite plot of diurnal rainfall variations in each regime: (1) strong westerly (SW) regime where the zonal wind exceeds mean plus standard deviation ($U \geq \bar{U} + \sigma$), (2) weak westerly (W) regime where the zonal wind is between 0 and mean plus standard deviation ($0 < U < \bar{U} + \sigma$), (3) weak easterly (E) regime where the zonal wind is between 0 and mean minus standard deviation ($\bar{U} - \sigma < U < 0$), and (4) strong easterly (SE) regime where the zonal wind is smaller than mean minus standard deviation ($U \leq \bar{U} - \sigma$).

The seasonal variations of the number of days falling into the four regimes (SW, W, E, and SE) defined above are shown in Figure 2b. During the boreal winter (December to March), the SW and W regimes are more dominant than the E and SE regimes. On the other hand, during the boreal summer (May to October), the E and SE regimes are more dominant than the SW and W regimes. We identified April and November as transient periods between the regimes, when the days of westerly wind (SW and W) are comparable to that of easterly wind (E and SE). The composite plots in the SW and W regimes may be considered to primarily represent the feature during the boreal winter, while the E and SE regimes are representative of the boreal summer.

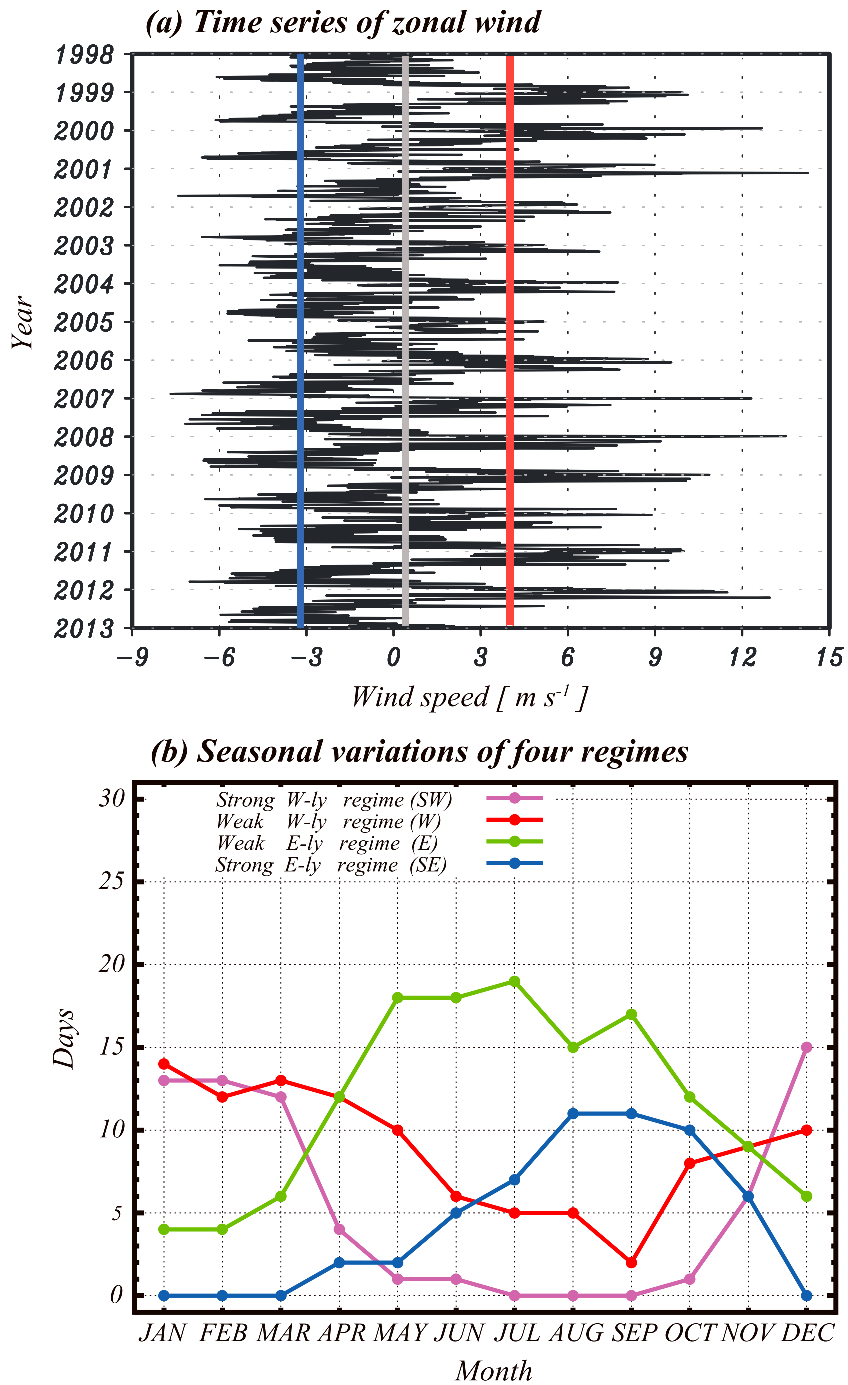

Figure 2. (a) Time series of the zonal wind averaged for the lower troposphere (1000–500 hPa) over the rectangular domain in Figure 1. The gray line shows the time mean of the time series $\bar{U}$, and the red and blue lines indicate the mean plus and minus standard deviation, respectively ($\bar{U}+\sigma$ and $\bar{U}-\sigma$), which are used as an index to identify four wind regimes (SW, strong westerly; W, weak westerly; E, weak easterly; SE, strong easterly). (b) Seasonal variations of the four wind regimes. The pink, red, green, and blue lines indicate the SW, W, E, and SE regimes, respectively.

3. Results

Figures 3a–3d show the time-longitude cross sections of composite surface precipitation from TRMM 2A25 for the rectangular area indicated by Figure 1 in each regime. In the SW regime (Figure 3a), the rainfall develops to the east of the island (104°E–106°E) from the evening to midnight local time (1800–0000 LT). The rainfall peak then migrates to the eastern offshore area (108°E–109°E) at about 8 m s^{-1}. It should be

10.1002/2016EA000181

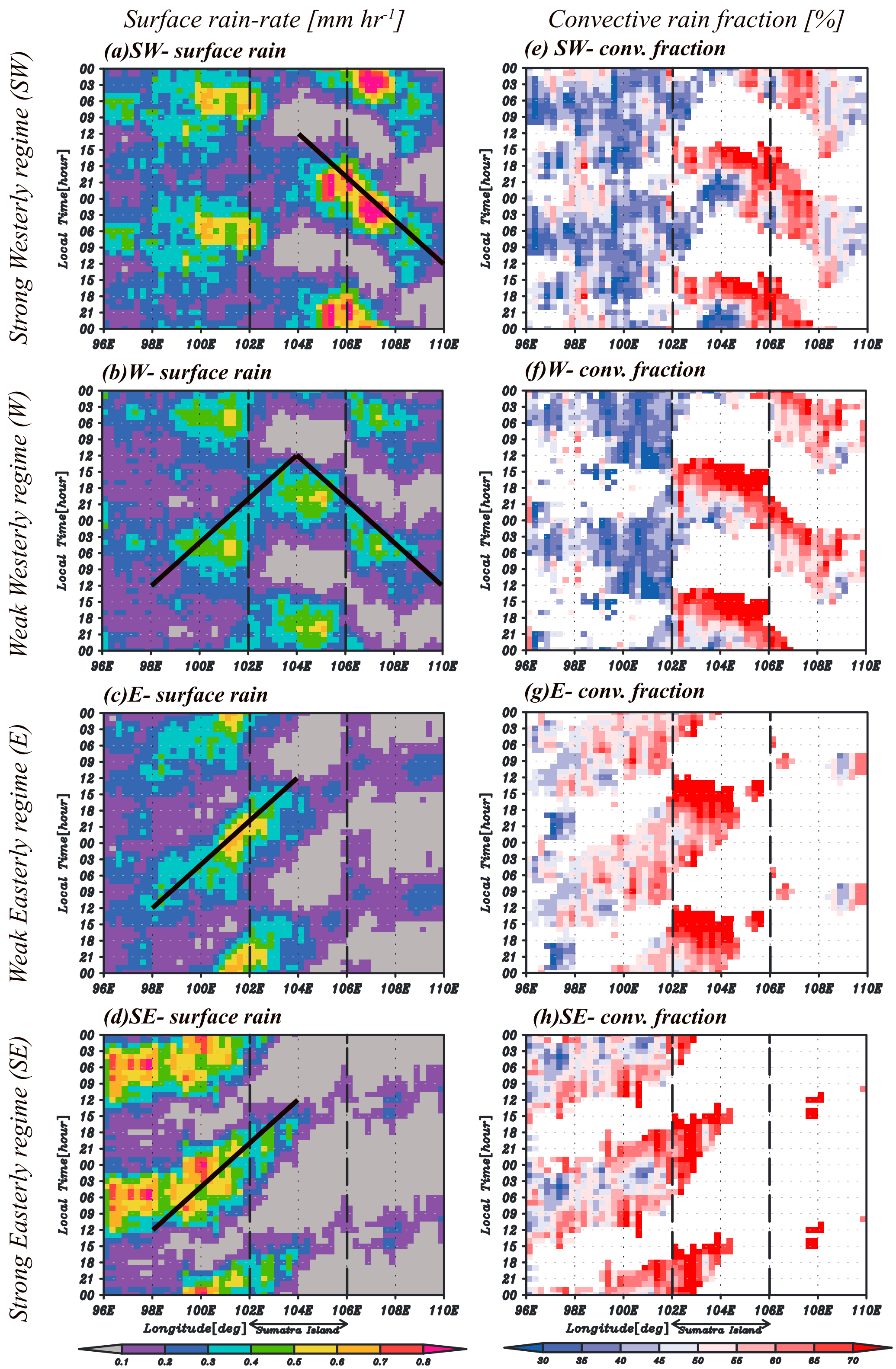

Figure 3. (a–d) Time-longitude cross sections of the composite surface rain rate and (e–h) the composite ratio to the total precipitation from TRMM 2A25 in SW (Figures 3a and 3e), W (Figures 3b and 3f), E (Figures 3c and 3g), and SE regimes (Figures 3d and 3h). The area between the two dashed lines from 102°E to 106°E corresponds to the land region. In Figures 3e–3h, the solid line indicates the subjectively estimated migration speed of 8 m s^{-1}. The area with surface rain rates below 0.2 mm h^{-1} is blanked out in Figures 3a–3d.

noted that the precipitation system redevelops when it arrives over the ocean east of the island (107°E) from midnight to early morning (0000–0300 LT). On the other hand, the westward propagation signal of a diurnal precipitation system is much weaker than the eastward propagation. The rainfall system over the ocean west of Sumatra Island (96°E–102°E) exhibits a notable development from early morning to midmorning (0300–0900 LT), although not completely vanishing during the rest of the day.

In the W regime (Figure 3b), rainfall systems are generated over the inland area (102°E–106°E) in the afternoon (1200–1500 LT) and intensify over the central part of the island (103°E–105°E) until evening (1800–2100 LT). Although the eastward migration signal is weaker in the W regime than in the SW regime, zonally symmetric propagation from the western coast to the Indian Ocean is found from the evening (1800–2100 LT) to the morning (0600–0900 LT) in the W regime. Both eastern and western migration systems redevelop off the coast (107°E and 101°E) from the evening to the morning (1800–0900 LT). The eastward and westward migrations have speeds of approximately 5 m s^{-1} and 4 m s^{-1}, respectively.

In the E regime (Figure 3c), rainfall is initiated over the western coast of the island (102°E–104°E) and develops from the evening to the early morning (1800–0300 LT), slightly earlier than in the W regime. After initiation, rain systems in this regime propagate solely to the west without any eastward counterparts. Similarly, a westward propagation is found in the SE regime (Figure 3d). However, rainfall in the SE regime grows in intensity continuously as it propagates farther off the western coast of the island (96°E–98°E). Propagation speeds in the E and SE regimes are estimated to be 8 m s^{-1} and 8–12 m s^{-1}, respectively. These results are qualitatively consistent with the outcomes using TRMM 2A12 TMI data (not shown).

Figures 3e to 3h show the time-longitude cross sections of the composite ratio of convective rain to total precipitation (sum of convective and stratiform rainfall). The eastward migrating systems in the SW and W regimes are characterized by convective rainfall. In contrast, the westward migrating systems in the SW and W regimes are dominated by stratiform rainfall. In the SW regime, stratiform rain almost entirely extends off the west coast of Sumatra Island throughout the day, except in the vicinity of 98°E from 1500 to 0000 LT. In the W regime, the migration signal of stratiform rainfall from the west coast of Sumatra Island (102°E) to the sea (100°E) is clearer than in the SW regime. In the westward propagating systems of the SE and E regimes, convective precipitation is more dominant than stratiform rainfall. However, convective rain gradually weakens as the precipitation system travels over the oceanic regions.

The sequences of the vertical profiles of the convective and stratiform reflectivity from TRMM 2A25 data are shown in Figure 4. In the SW regime (Figure 4a), intense convective rain systems with a deep structure develop in the evening (1800 LT) over the eastern portion of the island (104°E–106°E). Convective systems, with their structure and intensity being maintained, propagate from land to the eastern sea (107°E) in the late night (0000 LT). Vertical structure and reflectivity intensity get lower and weaker in the morning (0600 LT). The sharp bright bands in stratiform systems, which form as an organized convective system matures, are shown at midnight (0000 LT) over 104°E–107°E. The stratiform rain systems also exist through the day off the western coast of Sumatra Island (96°E–102°E). It especially enhances the intensity and yields the bright band structure in the morning (0600 LT) over 96°E–102°E and at noon (1200 LT) over 98°E–100°E.

In the W regime (Figure 4b), penetrating convective rainfall develops over 102°E–106°E in the evening (1800 LT). It propagates eastward and gradually weakens from midnight (0000 LT) to morning (0600 LT). Although moderate stratiform rain persists throughout the day off the western coast of Sumatra Island (96°E–102°E), deep stratiform rain with bright bands develops in the evening (1800 LT) over 103°E–105°E. It migrates westward, and the intensity of stratiform rain increases from the evening (1800 LT) over 103°E–105°E to the morning (0600 LT) over 99°E–102°E.

In the E regime (Figure 4c), deep convective rain takes place in the evening (1800 LT) over 102°E–105°E and the rain system gradually weakens from midnight (0000 LT) over 100°E–103°E to the morning (0600 LT) over 99°E–101°E. Stratiform rainfall with bright band structures occurs over the western coast of Sumatra Island (101°E–103°E) in the evening (1800 LT) and then matures during the night (00 LT) over 100°E–102°E. It propagates westward, maintaining its structure from the evening (1800 LT) over 101°E–103°E to noon (1200 LT) over 97°E–99°E.

In the SE regime (Figure 4d), the penetrating convective rainfall system develops in the evening (1800 LT) over 101°E–104°E and propagates westward with upkeep of strong reflectivity intensity and its tall structure.

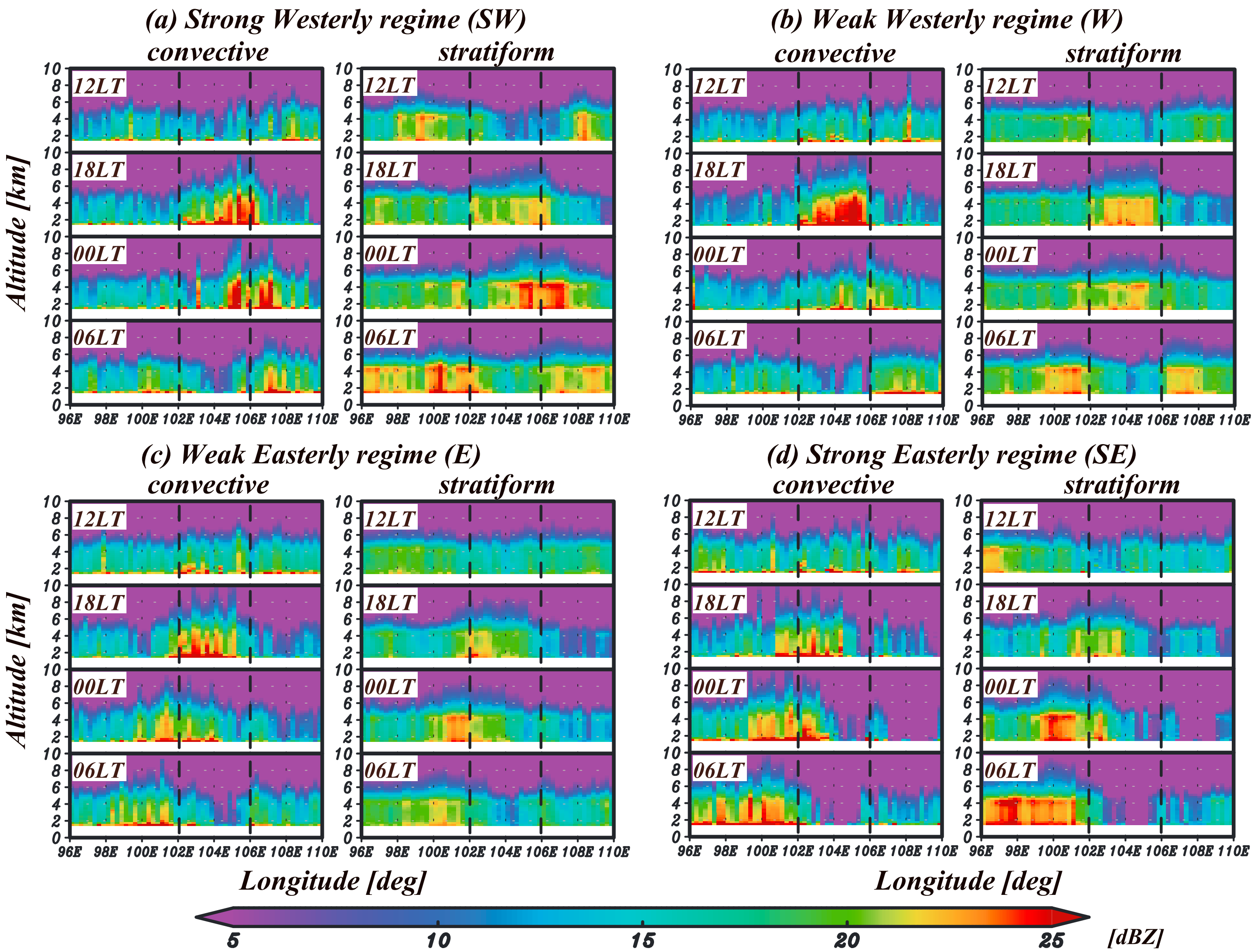

Figure 4. The sequence of the vertical distributions of the (left) convective and (right) stratiform reflectivity from TRMM 2A25 in the (a) SW, (b) W, (c) E, and (d) SE regimes. The area between the two dashed lines at 102°E and 106°E corresponds to the land region.

The deep stratiform rainfall, which occurs in the evening (1800 LT) over 101°E–104°E with the bright band, gradually becomes stronger from the evening (1800 LT) over 101°E–104°E to noon (1200 LT) over 96°E–97°E and maintains its bright band structure.

4. Discussion

4.1. Seasonality of Diurnal Rainfall Migration

As mentioned in the previous section, it was shown that the direction of diurnal rainfall propagation is related to the direction of ambient zonal wind. In this section, the seasonal variations of diurnal precipitation migration are discussed in terms of propagation direction. To this end, we equally divide the year into four periods into a seasonal-mean composite plot in a similar manner to Figures 3a–3d (Figure 5). The four periods are December, January, and February (DJF; Figure 5a); March, April, and May (MAM; Figure 5b); June, July, and August (JJA; Figure 5c); and September, October, and November (SON; Figure 5d).

In DJF (Figure 5a), rainfall systems occur in the noon (1200 LT) over land (102°E–106°E) and propagate both eastward and westward. The eastward propagation of diurnal rainfall is similar to the result in the SW and W regimes (Figures 3a and 3b), while the westward migration is associated with the W and E regimes

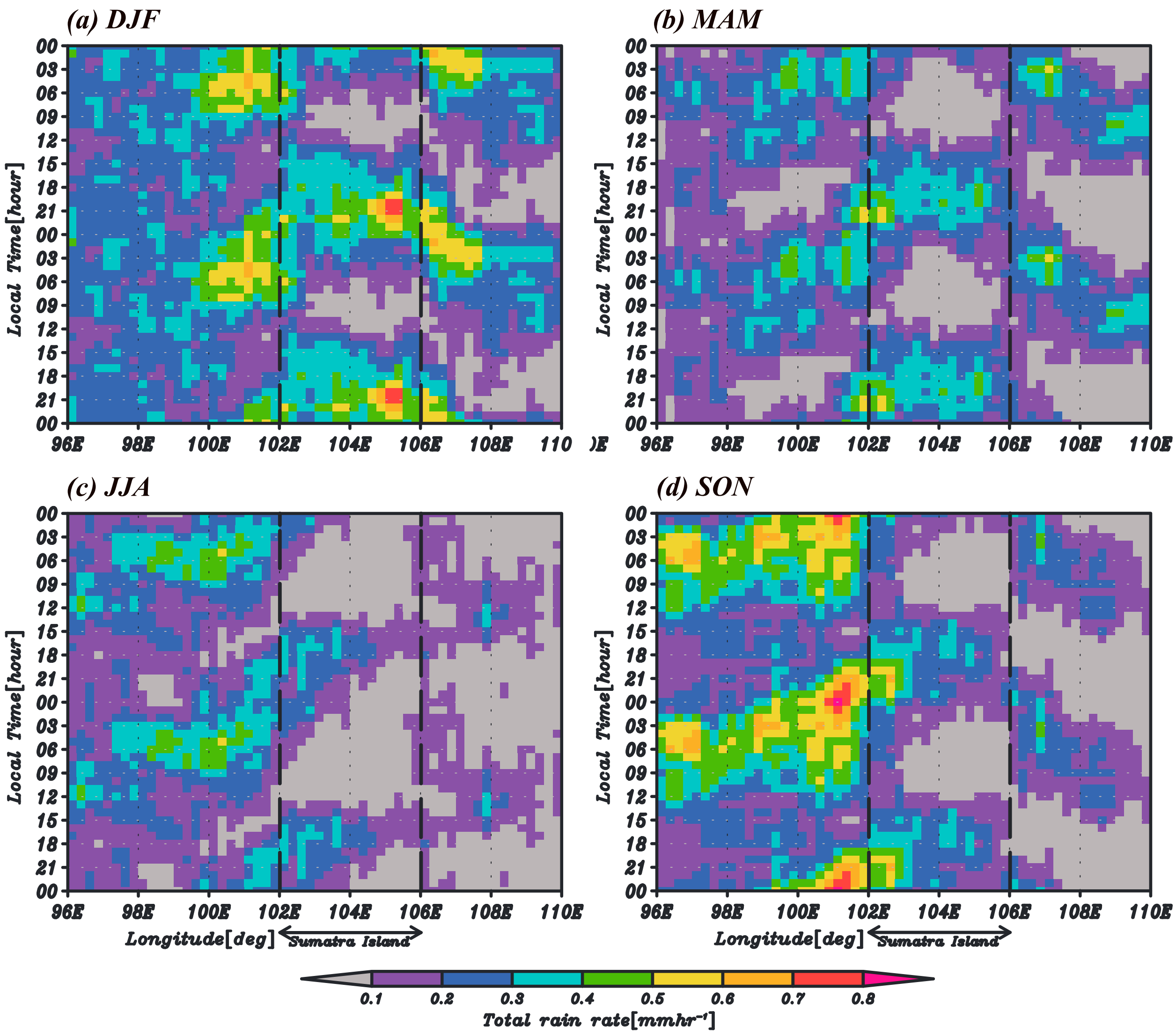

Figure 5. Time-longitude cross sections of the composite surface rain rate from TRMM 2A25 for (a) December, January, and February; (b) March, April, and May; (c) June, July, and August; and (d) September, October, and November.

(Figures 3b and 3c). Figure 2b shows that this period (DJF) is dominated by the SW and W regimes with a secondary contribution of the E regime.

In MAM (Figure 5b), the rainfall extends over land (102°E–106°E) from noon to midnight (1200–0000 LT) and simultaneously migrates to the east and west with an amplitude overall weaker than in DJF (Figure 5a). This propagation direction and its characteristics might be interpreted as a combination of the W and E regimes (Figures 3b and 3c). This is supported by Figure 2b, showing that MAM is dominated by the W and E regimes with the exception of March, for which the SW regime makes a comparable contribution. *Mori et al.* [2004] also show that diurnal precipitation migrates eastward and westward as seen in Figures 5a and 5b of this study.

In JJA (Figure 5c), rainfall systems over the western portion of the island (102°E–104°E) in the afternoon and evening (1500–2100 LT) migrate westward only. The propagation signal is as observed in the E regime (Figure 3c), although weaker in strength. These characteristics of the direction of diurnal precipitation migration are as expected, given that the E regime dominates in this period (Figure 2b).

In SON (Figure 5d), precipitation systems generated from the west coast to the land (102°E–106°E) propagate to the east and west. The westward propagation signal, extending over a distance from the starting location (96°E–98°E), is especially stronger than the eastward one. It should be noted that its westward signal appears to be composed of two propagation speeds (slower and faster), presumably explained by a mixture of the E and SE regimes (Figures 3c and 3d). The weak eastward propagation may be ascribed to the W regime, which gradually becomes more frequent as time proceeds in the second half of the SON period (Figure 2b).

Based on these results, the seasonality of the diurnal propagation is interpretable in terms of the seasonally changing proportion of the different wind regimes as implied in Figure 2. These results are consistent with the seasonality of diurnal cloud migration reported by *Sakurai et al*. [2005].

4.2. Comparison Between Diurnal Rainfall Propagation and Zonal Wind Speed

The relationship between diurnal rainfall propagation and ambient zonal wind was qualitatively shown in sections 3 and 4.1. In this section, we quantitatively compare the propagation speeds with the zonal wind speed (Figure 6) and discuss possible migration mechanisms.

In the SW regime, the wind is westerly from 1000 hPa to 400 hPa (Figure 6a) and the wind speed from 800 hPa to 600 hPa matches the migration speed (approximately 8 m s^{-1}) of the tall convective precipitation systems (Figures 3a and 4a). It is suggested that the eastward propagation of diurnal rainfall dominated by convective rain may be primarily owing to the lower level (800–600 hPa) background wind in the SW regime.

In the W regime, the eastward migration speed (approximately 5 m s^{-1}) of convective rainfall systems (Figure 3f) is slightly faster than the wind speed (approximately 0–4 m s^{-1}) in the lower troposphere (1000–500 hPa) (Figure 6b). Thus, simple advection by lower level wind cannot completely account for convection migration speed. The difference in speeds (1–2 m s^{-1}) might be insignificant taking into account the horizontal resolutions of the reanalysis data, local circulation, and uncertainty about estimated propagation speed. Westward migration of stratiform rainfall (about 4 m s^{-1}), on the other hand, is completely opposite of wind direction in the lower troposphere (1000–500 hPa) in the W regime. Therefore, it is unlikely that advection by the lower level wind (1000–500 hPa) is critical for the movement of stratiform rain systems. In this regime, however, wind is easterly above 500 hPa (Figure 6b) and the composite wind speed for 400–250 hPa (about 3–6 m s^{-1}) agrees with the migration speed (about 4 m s^{-1}) of deep stratiform rain (Figure 4b). It is suggested that the maximum peak, which rainfall systems redevelop over the sea (101.5°E) in the morning (0600 LT) in Figure 3b, might be caused by local effects (e.g., land-sea breeze). On the other hand, the weak signal of westward diurnal rainfall migration that dominates stratiform rainfall is shown from 1800 LT to 0600 LT. It might be suggested that the precipitation system, produced by local circulation over the west coast, is strengthened by merging with the stratiform rainfall system driven by the ambient wind from land to sea in the mid-upper troposphere. Hence, we speculate that the wind in the mid-upper troposphere may play a role in the westward migration of rainfall systems.

In the E regime, the westward propagation speed (about 8 m s^{-1}) of convective precipitation is comparable to that reported by *Mori et al*. [2004]. In this regime, the speed of the composite zonal wind is less than 4 m s^{-1} in the lower (1000–500 hPa) level (Figure 6c), which is much slower than migration speed. It is unlikely that the westward propagation is mostly controlled by the lower tropospheric wind, although we cannot completely exclude the possibility that a zonally nonhomogeneous local circulation accelerates the westward advection associated with ambient flow in the lower level. On the other hand, the speed of about 8 m s^{-1} corresponds to the zonal wind in the 400–250 hPa levels (Figure 6c). The rainfall system is composed of not only convective-type rainfall but also stratiform-type rainfall (Figure 4c). Thus, the advection of stratiform precipitation by the mid-upper level wind might be partly responsible for the westward movement of the precipitation system.

In the SE regime, the westward propagation speed (approximately 8–12 m s^{-1}) of convective rainfall is the fastest among all regimes. In this case, we found the relationship between the movement of the system and ambient zonal wind to be similar to those in the E regime. The propagation speed exceeds that of the composite zonal wind in the lower (1000–500 hPa) troposphere (less than 6 m s^{-1}) and better agrees with that in the mid-upper (500–200 hPa) troposphere (Figure 6d). Therefore, we also speculate that mid-upper level wind may play an essential role in the westward movement of rainfall systems.

Sakurai et al. [2009] investigated the propagation of diurnal cloud systems over Sumatra Island based on a case study by using intensive observation (CPEA-I) data. They discovered diurnal cloud systems with a horizontal scale of several hundred kilometers propagating eastward and westward and that cloud system directions are parallel to lower troposphere zonal wind. The relationship between the convective-type diurnal

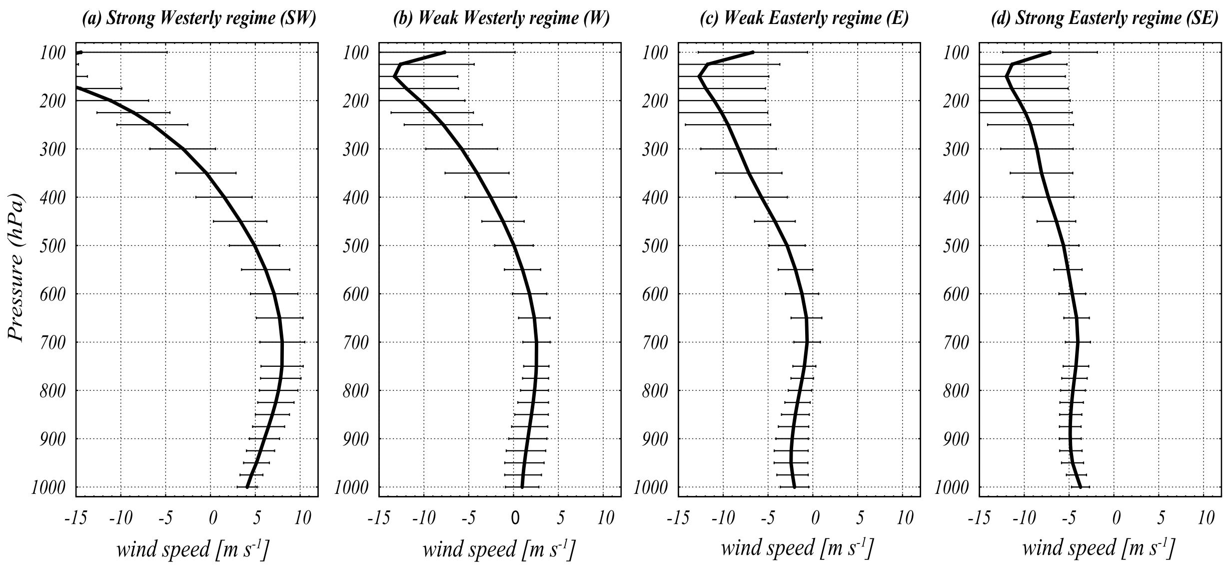

Figure 6. Vertical profiles of the zonal wind averaged over the rectangular domain of Figure 1 for (a) SW, (b) W, (c) E, and (d) SE regimes. Error bars indicate one standard deviation at each level.

rainfall propagation directions and ambient wind in the lower troposphere (1000–500 hPa) is consistent with our findings.

Note that westward-propagating systems redevelop off the western coast in the W, E, and SE regimes (Figures 3b–3d). Some previous studies suggest that cold pool dynamics are important to the redevelopment of rainfall systems over the ocean [*Sakurai et al.*, 2009, 2011; *Fujita et al.*, 2010]. Cold pools, however, are associated with intense downdrafts produced in the convective core [*Feng et al.*, 2015]. Although the stratiform rainfall areas dominate the convective areas over the ocean west of Sumatra Island, convective rainfall coexists (Figures 3e–3h), which might be critical to maintain systems over the ocean [*Moteki et al.*, 2008]. On the other hand, the importance of local effects also has been discussed in some previous studies [*Wu et al.*, 2009; *Sakurai et al.*, 2011; *Fujita et al.*, 2013]. They suggest that mountainous topography and thermally induced local circulation can play an important role in the organization of heavy rainfall during the night over the west coast of Sumatra Island. *Wu et al.* [2009] uses numerical models to show that heavy nighttime rainfall is caused by offshore flow from mountainous topography and convection. These local effects may explain aspects of the redevelopment of rainfall systems off the west coast (e.g., 101°E at 0600 LT in the W regime) as found in this study.

The "feeder-seeder" mechanism [*Locatelli et al.*, 1983] also seems like a plausible explanation for the westward propagation of precipitation systems and their redevelopment over the ocean, which is schematically shown in Figure 12 of *Mori et al.* [2004]. The feeder related to the low-level clouds off the coast of western mountainous region is enhanced by receiving the seeder associated with the stratiform clouds (e.g., anvil cloud) in the mid-upper (500–200 hPa) troposphere advected by the ambient wind. As we focus on the different aspects, wave dynamics have been discussed by previous studies, e.g., gravity waves associated with upper level heating and lower level cooling of the stratiform rainfall [*Mapes*, 2000] or induced by diurnal heating of the daytime mixed layer on land [*Mapes et al.*, 2003]. The propagation speeds of their results are 20 m s^{-1} and 15 m s^{-1}, respectively. In this study, we have found no evidence implying that the propagation of rainfall systems agrees with the gravity wave speed and do not explore this possibility further.

These discussions suggest that a probable mechanism of the eastward migrating systems characterized by convective-type rain is the advection by background wind in the lower troposphere and/or self-replication of convective systems associated with the diurnal cycle. The same mechanism may be at work with respect to the westward propagation of stratiform-type precipitation. However, the mechanism of westward propagating systems characterized by convective rainfall remains unclear in our study. Although the background wind seems important in the migration direction of diurnal cloud systems with precipitation, an assessment of other aspects of dynamical and thermodynamic elements needs to be investigated by making use of a numerical model of intense observations with a long enough time span in future work.

5. Conclusion

This study investigates the climatological relationship between the direction of diurnal rainfall migration and ambient wind over southern Sumatra Island by using long-term data (15 years) from TRMM-PR satellite observation and reanalysis.

In the strong westerly (SW) regime, diurnal convective-type rainfall propagates to the east and its speed is consistent with lower level tropospheric wind (800–600 hPa). In the weak westerly (W) regimes, convective diurnal rainfall migrates eastward, although its signal is weaker than in the SW regime. In contrast, diurnal stratiform-dominated rainfall propagates westward in association with easterly background wind in the mid-upper troposphere. On the other hand, in the weak easterly (E) and strong easterly (SE) regimes, the convective and stratiform rainfall associated with the diurnal cycle migrate only to the west. The propagation speed of the diurnal rainfall matches the wind speed in the mid-upper level in each regime. The advection of stratiform precipitation by the mid-upper level wind might be partly responsible for the westward movement of precipitation systems.

Based on these results, the direction of diurnal rainfall migration appears to be generally consistent with ambient zonal wind. Although some features have been reported by previous studies [*Mori et al*., 2004; *Sakurai et al*., 2005; *Sakurai et al*., 2009], this is the first study to report the propagation direction of diurnal rainfall systems through a whole year over Sumatra Island.

Acknowledgments
The TRMM 2A25 product was provided by the Japan Aerospace Exploration Agency. TRMM 3G68 product information can be found at ftp://trmmopen.gsfc.nasa.gov/pub. TRMM 3B42 product was distributed by NASA Goddard Earth Sciences Data and Information Services Center. ERA Interim data were provided by ECMWF (https://climatedataguide.ucar.edu/climate-data/era-interim). This work is partly supported by the Japan Society for the Promotion of Science Grant-in-Aid (KAKENHI) for Grant-in-Aid for Scientific Research (B) (26287113) and for Challenging Exploratory Research (26610150). The authors thank anonymous reviewers for providing positive comments for improvement of this paper.

References

Feng, Z., S. Hagos, A. K. Rowe, C. D. Burleyson, M. N. Martini, and S. P. de Szoeke (2015), Mechanisms of convective cloud organization by cold pools over tropical warm ocean during the AMIE/DYNAMO field campaign, *J. Adv. Model. Earth Syst.*, *7*, 357–381, doi:10.1002/2014MS000384.

Fujita, M., F. Kimura, and M. Yoshizaki (2010), Morning precipitation peak over the Strait of Malacca under a calm condition, *Mon. Weather Rev.*, *138*, 1474–1486.

Fujita, M., H. G. Takahashi, and M. Hara (2013), Diurnal cycle of precipitation over the eastern Indian Ocean off Sumatra Island during different phases of Indian Ocean Dipole, *Atmos. Sci. Lett.*, *14*, 153–159.

Hendon, H., and K. Woodberry (1993), The diurnal cycle of tropical convection, *J. Geophys. Res.*, *98*, 16,623–16,637, doi:10.1029/93JD00525.

Houze, R. A., Jr., S. G. Geotis, F. D. Marks, and A. K. West (1981), Winter monsoon convection in the vicinity of north Borneo. Part I: Structure and time variation of the clouds and precipitation, *Mon. Weather Rev.*, *109*, 1595–1614.

Ichikawa, H., and T. Yasunari (2006), Time-space characteristics of diurnal rainfall over Borneo and surrounding oceans as observed by TRMM-PR, *J. Clim.*, *19*, 1238–1260.

Ichikawa, H., and T. Yasunari (2008), Intraseasonal variability in diurnal rainfall over New Guinea and the surrounding oceans during austral summer, *J. Clim.*, *21*(12), 2852–2868.

Kikuchi, K., and B. Wang (2008), Diurnal precipitation regimes in the global tropics, *J. Clim.*, *21*(11), 2680–2696.

Locatelli, J. D., P. V. Hobbs, and K. R. Biswas (1983), Precipitation from stratocumulus clouds affected by fallstreaks and artificial seeding, *J. Appl. Meteorol. Climatol.*, *22*, 1393–1403.

Love, B. S., A. J. Matthews, and G. M. S. Lister (2011), The diurnal cycle of precipitation over the Maritime Continent in a high resolution atmospheric model, *Q. J. R. Meteorol. Soc.*, *137*, 934–947.

Mapes, B. E. (2000), Convective inhibition, subgridscale triggering, and stratiform instability in a toy tropical wave model, *J. Atmos. Sci.*, *57*, 1515–1535.

Mapes, B. E., T. T. Warner, and M. Xu (2003), Diurnal patterns of rainfall in northwestern South America. Part III: Diurnal gravity waves and nocturnal convection offshore, *Mon. Weather Rev.*, *131*, 830–844.

Mori, S., J.-I. Hamada, Y. I. Tauhid, M. D. Yamanaka, N. Okamoto, F. Murata, N. Sakurai, H. Hashiguchi, and T. Sribimawati (2004), Diurnal land-sea rainfall peak migration over Sumatera Island, Indonesian Maritime Continent observed by TRMM satellite and intensive rawinsonde soundings, *Mon. Weather Rev.*, *132*, 2021–2039.

Moteki, Q., et al. (2008), Mechanism of the northward propagation of mesoscale convective systems observed on 15 June 2005 during PALAU2005, *J. Geophys. Res.*, *113*, D14126, doi:10.1029/2008JD009793.

Neale, R., and J. Slingo (2003), The Maritime Continent and its role in the global climate: A GCM study, *J. Clim.*, *16*, 834–848.

Nesbitt, S. W., and E. J. Zipser (2003), The diurnal cycle of rainfall and convective intensity according to three years of TRMM measurements, *J. Clim.*, *16*, 1456–1475.

Nitta, T., and S. Sekine (1994), Diurnal variation of convective activity over the tropical western Pacific, *J. Meteorol. Soc. Japan*, *72*, 627–641.

Ohsawa, T., H. Ueda, T. Hayashi, A. Watanabe, and J. Matsumoto (2001), Diurnal variations of convective activity and rainfall in tropical Asia, *J. Meteorol. Soc. Japan*, *79*, 333–352.

Ramage, C. S. (1968), Role of a tropical "Maritime Continent" in the atmospheric circulation, *Mon. Weather Rev.*, *96*, 365–369.

Sakurai, N., F. Murata, M. D. Yamanaka, S. Mori, J.-I. Hamada, H. Hashiguchi, Y.-I. Tauhid, T. Sribimawati, and B. Suhardi (2005), Diurnal cycle of cloud system migration over Sumatera Island, *J. Meteorol. Soc. Japan*, *83*, 835–850.

Sakurai, N., et al. (2009), Internal structures of migratory cloud systems with diurnal cycle over Sumatera Island during CPEA-I campaign, *J. Meteorol. Soc. Japan*, *87*, 157–170.

Sakurai, N., et al. (2011), Migration process and 3D wind field of precipitation systems associated with a diurnal cycle in west Sumatera: Dual Doppler radar analysis during the HARIMAU2006 campaign, *J. Meteorol. Soc. Japan*, *89*, 341–361.

Wu, P., M. Hara, J. Hamada, M. D. Yamanaka, and F. Kimura (2009), Why a large amount of rain falls over the sea in the vicinity of western Sumatra Island during nighttime, *J. Appl. Meteorol. Climatol.*, *48*, 1345–1361.

Yang, G.-Y., and J. Slingo (2001), The diurnal cycle in the Tropics, *Mon. Weather Rev.*, *129*, 784–801.